

ESI of

Oxidation of HOSO[•] by O₂ (³Σ_g⁻): A key reaction deciding the fate of HOSO[•] in the atmosphere

Philips Kumar Rai, Saptarshi Sarkar, Biman Bandyopadhyay,* and Pradeep
Kumar*

*Department of Chemistry, Malaviya National Institute of Technology Jaipur, Jaipur,
302017, India*

E-mail: biman.chy@mnit.ac.in; pradeep.chy@mnit.ac.in

Sl. No.	Contents
1.	Table S1: Comparison of frequencies (in cm^{-1}) and geometrical parameters of the isolated species, obtained in present work (MN15L/aug-cc-pV(T+d)Z) and at other methods (MP2/aug-cc-pV(T+d)Z and M06-2X/aug-cc-pV(T+d)Z) with the experimental and higher level theoretical data available in literature.
2.	Table S2: T1 diagnostic values for each species involved in the reaction.
3.	Figure S1: Gibbs free energy profile for $\text{HOSO}^\bullet + \text{O}_2$ (${}^3\Sigma_g^-$) reaction obtained at CCSD(T)/CBS level of theory at 298 K.
4.	Table S3: Pressure dependence bimolecular rate constants $k(T)$ in $\text{cm}^3 \text{molecule}^{-1} \text{s}^{-1}$ for $\text{HOSO}^\bullet + \text{O}_2$ (${}^3\Sigma_g^-$) reaction within temperature range of 213-400 K.
5.	Table S4: Cartesian coordinates and all normal mode frequencies of the optimized geometries calculated at MN15L/aug-cc-pV(T+d)Z level of theory.
6.	Table S5: Topological properties of the bond critical points of the three species; RC, TS1 and PC involved in the reaction.
7.	Figure S2: IRC for the transition state (TS1) of the title reaction obtained at MN15L/aug-cc-pV(T+d)Z level of theory.
8.	Figure S3: Potential energy surface for $\text{HOSO}^\bullet + \text{O}_2$ (${}^1\Delta_g$) reaction after including post-CCSD(T) corrections.
9.	Table S6: The bimolecular rate constants ($k(T)$), k_{eff} and $t_{1/2}$ for $\text{HOSO}^\bullet + \text{O}_2$ (${}^1\Delta_g$).
10.	Table S7: The rate constant values for $\text{HOSO}^\bullet + \text{O}_2$ (${}^3\Sigma_g^-$) reaction with rigid rotor treatment (k_{WTHR}) along with hindered rotor treatment (k_{HR}).
11.	Table S8: The rate constant values for $\text{HOSO}^\bullet + \text{O}_2$ (${}^3\Sigma_g^-$) reaction through TS2 using TST/ZCT method.

Table S1: Comparison of frequencies (in cm^{-1}) and geometrical parameters of the isolated species, obtained in present work (MN15L/aug-cc-pV(T+d)Z) and at other methods (MP2/aug-cc-pV(T+d)Z and M06-2X/aug-cc-pV(T+d)Z) with the experimental and higher level theoretical data available in literature.

Methods	Species	Frequencies (in cm^{-1})		Bond lengths (\AA)					Angles ($^{\circ}$)				$D_{O=S-O-H}$
		R_{O-H}	$R_{O=O}$	R_{O-O}	R_{S-O}	$R_{S=O}$	A_{O-O-H}	$A_{O=S=O}$	$A_{O=S-O}$	A_{H-O-S}			
Experimental	O_2 (${}^3\Sigma_g^-$)	1580		1.21					119.5				
	SO_2	526	1168	1381				1.43					
	HO_2^*	1098	1392	3436	0.97	1.33			104.3				
ROCCSD(T)/cc-pV(5+d)Z	planar syn-HOSO *	389	784	1055	0.97		1.63	1.47			108.3	107.9	0.0
ROCCSD(T)/cc-pV(5+d)Z	planar anti-HOSO *	1184	3576		0.97		1.64	1.46			105.3	108.2	180.0
ROCCSD(T)/cc-pV(T+d)Z	non-planar syn-HOSO *				0.97		1.64	1.47			108.8	107.2	24.2
MN15L/aug-cc-pV(T+d)Z	O_2 (${}^3\Sigma_g^-$)	1681.6		1.21					119.0				
	SO_2	537	1229	1436			1.43						
	HO_2^*	1200	1463	3645	0.97	1.32			105.2				
	planar syn-HOSO *	321	402.3	828.8	0.97		1.62	1.47			108.4	107.8	1.9
	planar anti-HOSO *	1099.9	1239.7	3791.3									
	planar anti-HOSO *	118.8	424.8	817.3	0.97		1.63	1.46			105.0	108.4	180.0
	non-planar syn-HOSO *	56.1	406.6	828.5	0.97		1.62	1.47			108.6	108.0	12.7
M06-2X/aug-cc-pV(T+d)Z	O_2 (${}^3\Sigma_g^-$)	1754.5		1.19					118.9				
	SO_2	540	1253	1453			1.43						
	HO_2^*	1253	1459.5	3688.8	0.97	1.31			105.8				
	planar syn-HOSO *	41.8	403.8	830.1	0.97		1.62	1.46			108.0	109.0	1.74
	planar anti-HOSO *	1081.5	1229.7	3787.3									
	planar anti-HOSO *	65.91	426.1	816.1	0.97		1.63	1.45			105.2	109.7	180.0
	non-planar syn-HOSO *	1071.3	1253.9	3822.8									0.0
MP2/aug-cc-pV(T+d)Z	O_2 (${}^3\Sigma_g^-$)	1454		1.22					119.7				
	SO_2	498	1119	1338.4			1.45						
	HO_2^*	1223	1449	3659	0.97	1.31			104.7				
	planar syn-HOSO *	150.6	383.9	802.0	0.97		1.63	1.47			108.9	107.0	1.0
	planar anti-HOSO *	1068.4	1267.2	3716.6									
	planar anti-HOSO *	144.1	411.9	786	0.97		1.64	1.46			106.0	108.1	180.0
	non-planar syn-HOSO *	1062	1338.8	3751.6									0.0
	non-planar syn-HOSO *	147.2	383.6	802	0.97		1.63	1.47			108.9	107.0	
		1068	1268	3717.3									

Table S2: T1 diagnostic values for each species involved in the reaction.

Species	T1 diagnostic
HOSO \bullet	0.0209
O ₂ ($^3\Sigma_g^-$)	0.0176
RC	0.0335
TS	0.0273
PC	0.0271
SO ₂	0.0209
HO $_2^\bullet$	0.0299

Figure S1: Gibbs free energy profile for $\text{HOSO}^\bullet + \text{O}_2$ (${}^3\Sigma_g^-$) reaction obtained at CCSD(T)/CBS level of theory at 298 K.

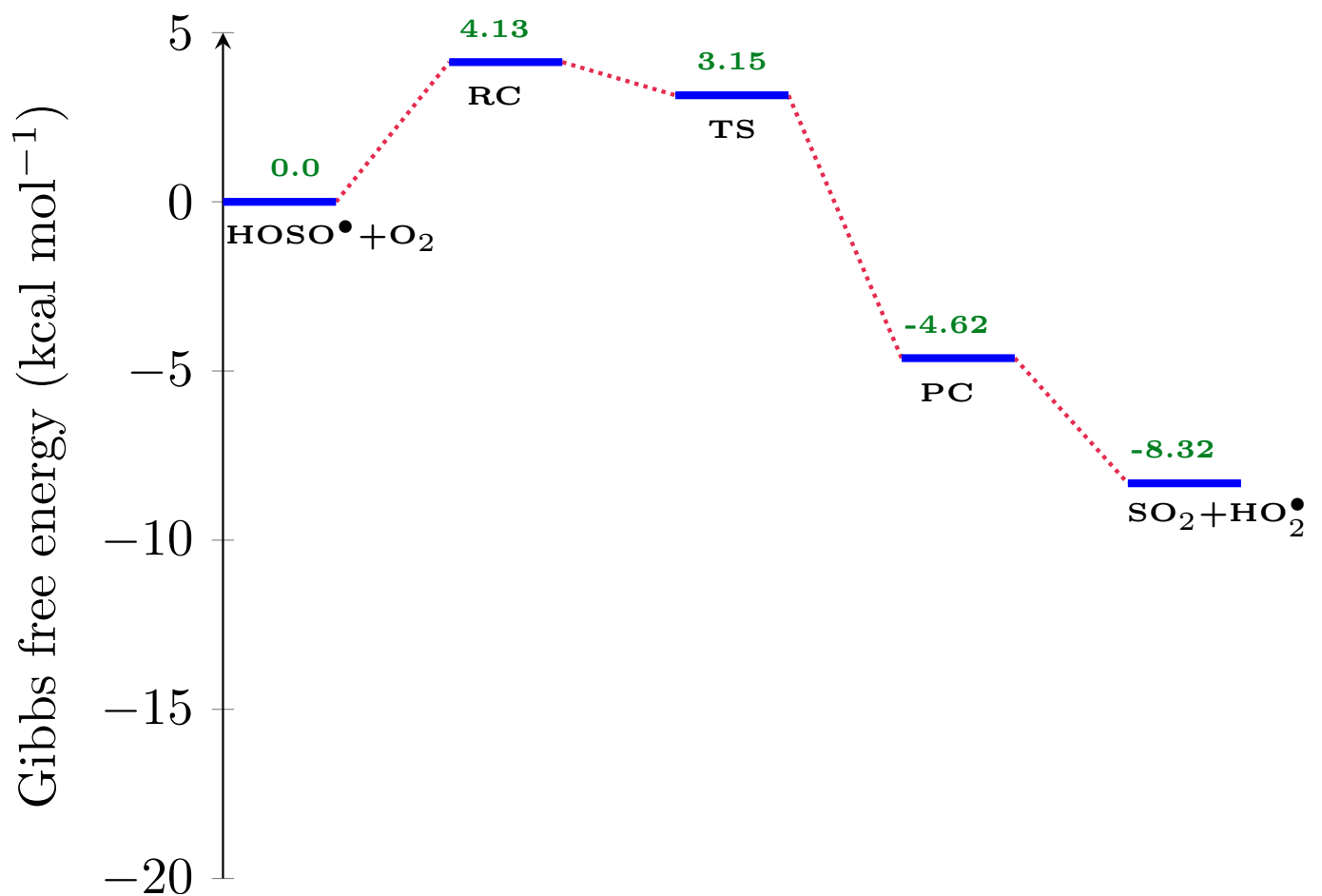


Table S3: Pressure dependence bimolecular rate constants $k(T)$ in $\text{cm}^3 \text{ molecule}^{-1} \text{ s}^{-1}$ for $\text{HOSO}^\bullet + \text{O}_2$ (${}^3\Sigma_g^-$) reaction within temperature range of 213-400 K obtained at CCSD(T)/CBS level of theory.

Temp (K)	Pressure (atm)				
	0.1	0.5	1.0	5.0	10.0
213	2.94×10^{-13}				
216	2.87×10^{-13}	2.87×10^{-13}	2.87×10^{-13}	2.87×10^{-13}	2.86×10^{-13}
219	2.80×10^{-13}	2.80×10^{-13}	2.80×10^{-13}	2.79×10^{-13}	2.79×10^{-13}
224	2.68×10^{-13}				
235	2.46×10^{-13}	2.46×10^{-13}	2.46×10^{-13}	2.45×10^{-13}	2.45×10^{-13}
250	2.20×10^{-13}	2.20×10^{-13}	2.20×10^{-13}	2.20×10^{-13}	2.19×10^{-13}
259	2.06×10^{-13}	2.06×10^{-13}	2.06×10^{-13}	2.05×10^{-13}	2.05×10^{-13}
260	2.05×10^{-13}	2.05×10^{-13}	2.05×10^{-13}	2.04×10^{-13}	2.03×10^{-13}
265	1.98×10^{-13}	1.98×10^{-13}	1.97×10^{-13}	1.97×10^{-13}	1.96×10^{-13}
270	1.91×10^{-13}	1.91×10^{-13}	1.91×10^{-13}	1.90×10^{-13}	1.89×10^{-13}
278	1.81×10^{-13}	1.81×10^{-13}	1.81×10^{-13}	1.80×10^{-13}	1.79×10^{-13}
280	1.79×10^{-13}	1.79×10^{-13}	1.79×10^{-13}	1.78×10^{-13}	1.77×10^{-13}
290	1.68×10^{-13}	1.68×10^{-13}	1.68×10^{-13}	1.67×10^{-13}	1.66×10^{-13}
298	1.59×10^{-13}	1.59×10^{-13}	1.59×10^{-13}	1.58×10^{-13}	1.57×10^{-13}
300	1.57×10^{-13}	1.57×10^{-13}	1.56×10^{-13}	1.55×10^{-13}	1.55×10^{-13}
310	1.48×10^{-13}	1.48×10^{-13}	1.48×10^{-13}	1.47×10^{-13}	1.45×10^{-13}
320	1.40×10^{-13}	1.40×10^{-13}	1.40×10^{-13}	1.38×10^{-13}	1.37×10^{-13}
350	1.19×10^{-13}	1.19×10^{-13}	1.19×10^{-13}	1.17×10^{-13}	1.15×10^{-13}
400	9.41×10^{-14}	9.33×10^{-14}	9.25×10^{-14}	9.01×10^{-14}	8.88×10^{-14}

Table S4: Cartesian coordinates and all normal mode frequencies of the optimized geometries calculated at MN15L/aug-cc-pV(T+d)Z level of theory.

Compound	Cartesian coordinate (Å)				Frequencies (cm ⁻¹)		
HOSO [•]	S	-0.134547	-0.478520	0.009617			
	O	-1.184717	0.545269	-0.012196	56.14	406.64	828.55
	O	1.308033	0.260965	-0.025750	1100.41	1239.26	3790.26
	H	1.166214	1.206443	0.149688			
O ₂	O	0.000000	0.000000	0.603041	1681.63		
	O	0.000000	0.000000	-0.603041			
RC	S	-0.740183	0.008989	-0.405436			
	O	-1.397849	-0.726807	0.638984	101.31	212.17	299.21
	O	-0.167537	1.360034	0.107436	367.08	465.33	587.99
	H	0.749462	1.177905	0.493786	645.80	949.21	1232.62
	O	1.087982	-0.777235	-0.334570	1307.96	1344.47	3056.80
	O	1.864087	-0.021209	0.337299			
TS1	S	-0.794665	0.050472	-0.402293			
	O	-1.493501	-0.687864	0.613350	-762.07	143.64	214.76
	O	-0.090744	1.286145	0.123334	343.28	486.55	572.24
	H	0.959482	0.946527	0.377946	795.15	1006.82	1142.28
	O	1.180466	-0.848087	-0.294249	1331.31	1378.65	1815.78
	O	1.873173	0.030546	0.314907			
TS2	S	1.471872	-0.318657	-0.133595			
	O	1.765468	1.074137	0.136478	-1370.59	26.89	82.87
	O	0.099313	-0.760150	0.350413	98.30	230.47	490.44
	H	-0.825447	-0.338063	-0.098757	672.86	990.74	1103.44
	O	-2.753060	0.254722	0.371496	1293.37	1422.18	1510.42
	O	-1.952284	0.110863	-0.578851			

PC	S	-0.967766	0.055251	-0.374850			
	O	-1.555000	-0.833277	0.584310	69.00	111.80	152.93
	O	-0.350206	1.265083	0.130575	251.30	303.60	532.38
	O	1.534336	-0.814497	-0.325915	549.02	1195.09	1260.94
	O	2.128732	0.165500	0.305543	1398.20	1532.20	3354.59
	H	1.421359	0.853500	0.441494			
SO_2	S	0.000000	0.000000	0.363728			
	O	0.000000	1.235372	-0.363728	537.12	1229.08	1436.92
	O	0.000000	-1.235372	-0.363728			
HO_2^{\bullet}	O	0.055586	0.716132	0.000000			
	O	0.055586	-0.607996	0.000000	1200.65	1463.72	3645.26
	H	-0.889383	-0.865087	0.000000			

Table S5: Topological properties of the bond critical points of the three species; RC, TS1 and PC involved in the reaction. The properties are determined from Bader topological analysis of the effective MN15L/aug-cc-pVTZ wave function and atom numbering refers to figure S4. [a] represents the density of all electrons ($e \text{ bohr}^{-3}$), [b]; Laplacian of electron density ($e \text{ bohr}^{-5}$), [c]; energy density (hartree bohr^{-3}), [d]; ellipticity of electron density and [e] represents the spin density of electrons.

Species	Bond	$\rho(r)^a$	$\nabla^2\rho(r)^b$	$E(r)^c$	ϵ^d	$\rho(s)^e$
RC	S1-O2	0.2995	1.2753	-0.3426	0.0985	0.0005
	S1-O5	0.1188	0.0029	-0.0587	0.0762	-0.0040
	O5-O6	0.4469	-0.2571	-0.4491	0.0125	-0.0027
	S1-O3	0.2400	0.5146	-0.2690	0.0231	-0.0001
	O6-H4	0.0583	0.1293	-0.0131	0.0598	-0.0017
	O3-H4	0.3051	-2.1540	-0.6109	0.0073	-0.0010
TS1	S1-O2	0.2985	1.2929	-0.3392	0.1274	0.0005
	S1-O5	0.0797	0.0929	-0.0215	0.0608	-0.0035
	O5-O6	0.4495	-0.2762	-0.4535	0.0256	-0.0030
	S1-O3	0.2569	0.7357	-0.2884	0.0662	-0.0001
	O6-H4	0.1448	-0.1458	-0.1169	0.0060	-0.0028
	O3-H4	0.2154	-0.8527	-0.3029	0.0039	-0.0019
PC	S1-O2	0.2995	1.3503	-0.3371	0.1496	0.0001
	S1-O4	0.0263	0.0785	0.0017	0.0822	-0.0015
	O4-O5	0.4093	-0.1635	-0.3740	0.0333	-0.0023
	S1-O3	0.2901	1.2085	-0.3259	0.1337	0.0000
	O5-H6	0.3362	-2.4753	-0.6815	0.0256	-0.0047
	O3-H6	0.0309	0.1066	0.0005	0.0355	-0.0007

Figure S2: IRC for the transition state (TS1) of the title reaction obtained at MN15L/aug-cc-pV(T+d)Z level of theory.

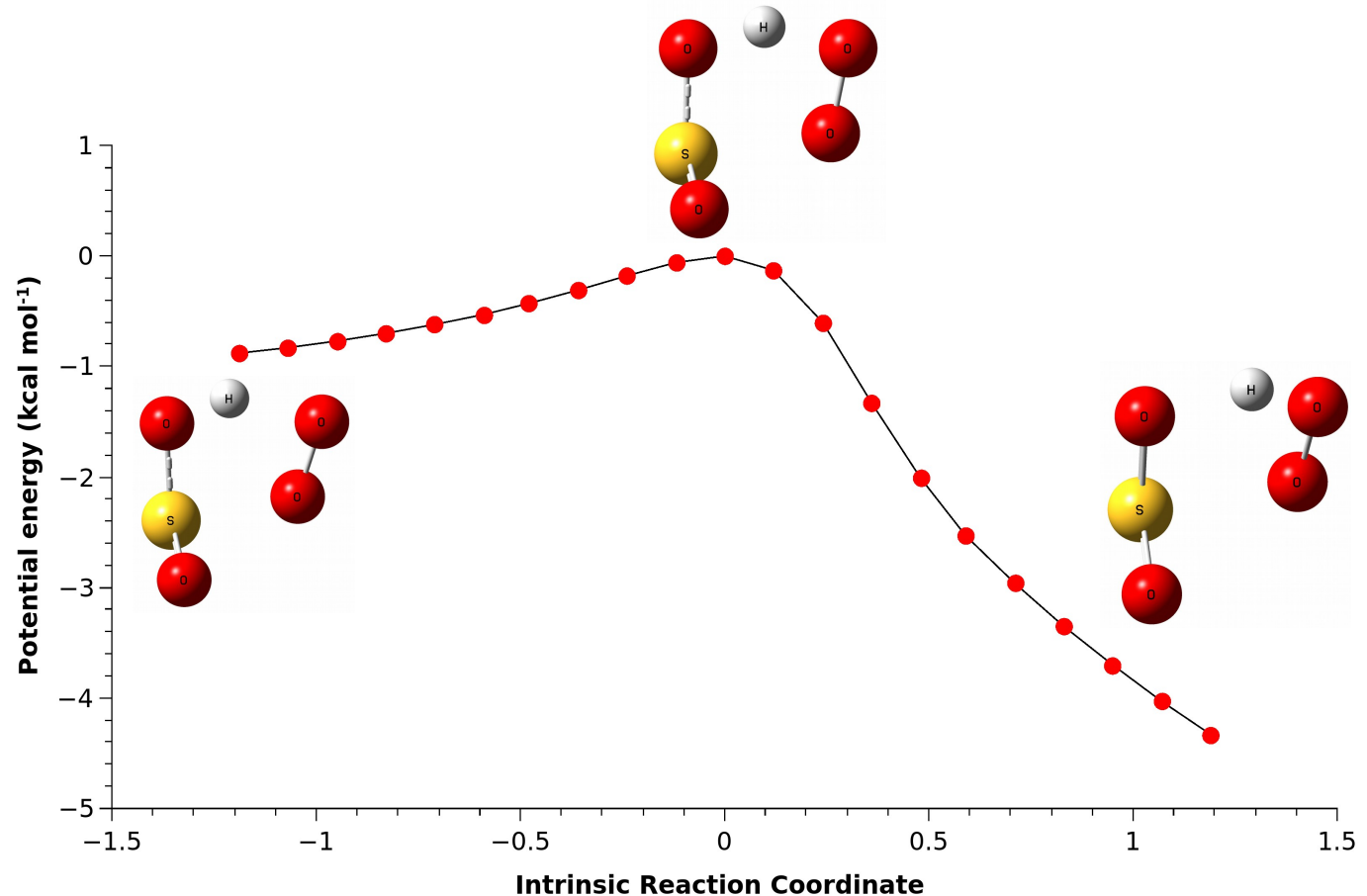


Figure S3: Potential energy surface for $\text{HOSO}^\bullet + \text{O}_2$ (${}^1\Delta_g$) reaction after including post-CCSD(T) corrections.

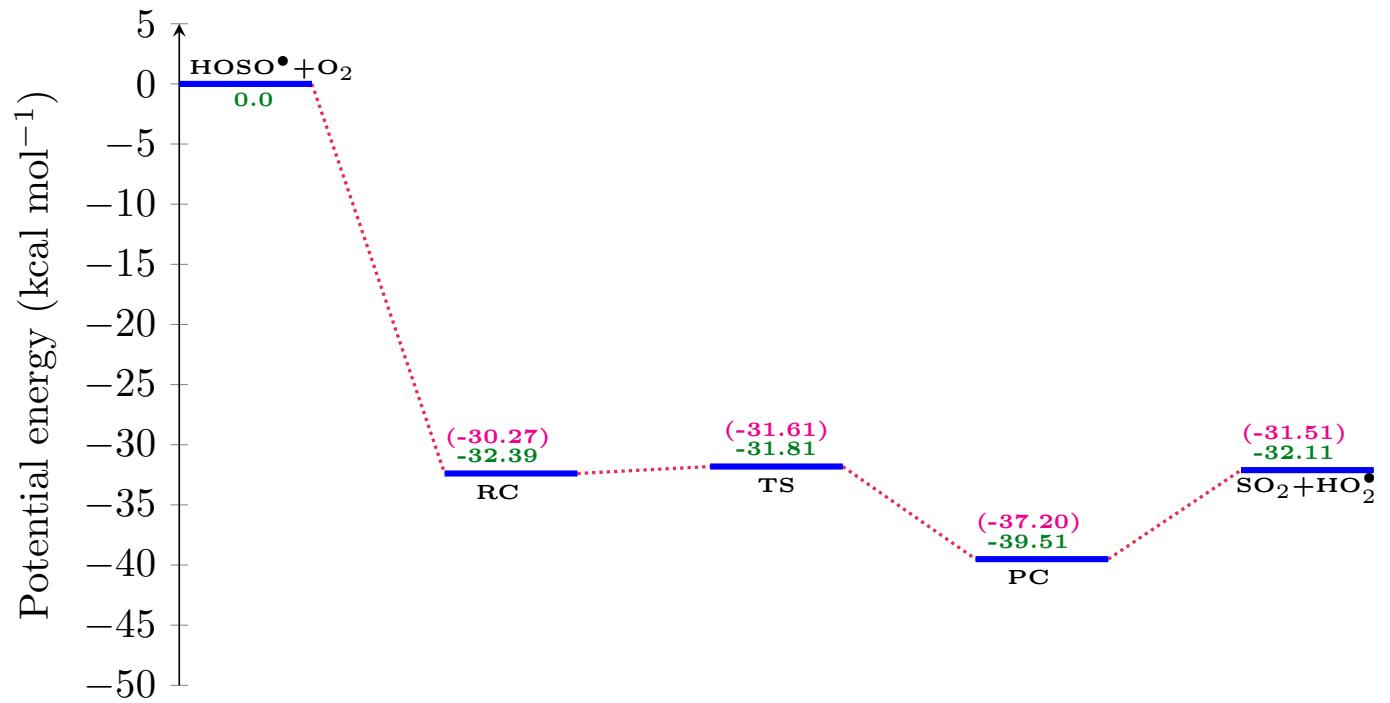


Table S6: The bimolecular rate constants ($k(T)$), effective rate constants (k_{eff}) and atmospheric lifetime ($t_{1/2}$) for $\text{HOSO}^\bullet + \text{O}_2$ (${}^1\Delta_g$). The values given for $k(T)$ and k_{eff} are in $\text{cm}^3 \text{molecule}^{-1} \text{s}^{-1}$ and $t_{1/2}$ is given in seconds.

T(K)	$k(T)$	k_{eff}	$t_{1/2}$
213	1.36×10^{-12}	6.80×10^{-1}	1.02×10^0
216	1.37×10^{-12}	6.84×10^{-1}	1.01×10^0
219	1.38×10^{-12}	6.89×10^{-1}	1.01×10^0
224	1.40×10^{-12}	6.98×10^{-1}	9.93×10^{-1}
235	1.44×10^{-12}	7.21×10^{-1}	9.61×10^{-1}
250	1.51×10^{-12}	7.54×10^{-1}	9.20×10^{-1}
259	1.54×10^{-12}	7.72×10^{-1}	8.98×10^{-1}
260	1.55×10^{-12}	7.77×10^{-1}	8.92×10^{-1}
265	1.57×10^{-12}	7.86×10^{-1}	8.82×10^{-1}
270	1.60×10^{-12}	8.00×10^{-1}	8.67×10^{-1}
278	1.64×10^{-12}	8.18×10^{-1}	8.47×10^{-1}
280	1.64×10^{-12}	8.22×10^{-1}	8.43×10^{-1}
290	1.70×10^{-12}	8.48×10^{-1}	8.17×10^{-1}
298	1.74×10^{-12}	8.68×10^{-1}	7.99×10^{-1}
300	1.74×10^{-12}	8.72×10^{-1}	7.95×10^{-1}
310	1.80×10^{-12}	8.99×10^{-1}	7.71×10^{-1}
320	1.85×10^{-12}	9.25×10^{-1}	7.49×10^{-1}
350	2.01×10^{-12}	1.01×10^0	6.88×10^{-1}
400	2.29×10^{-12}	1.14×10^0	6.06×10^{-1}

Table S7: The rate constant values for $\text{HOSO}^\bullet + \text{O}_2$ (${}^3\Sigma_g^-$) reaction with rigid rotor harmonic approximation (k_{WTHR}) along with hindered rotor approximation (k_{HR}). The values are given in $\text{cm}^3 \text{molecule}^{-1} \text{s}^{-1}$.

T(K)	k_{WTHR}	k_{HR}
213	3.17×10^{-13}	3.17×10^{-13}
216	3.09×10^{-13}	3.09×10^{-13}
219	3.02×10^{-13}	3.01×10^{-13}
224	2.90×10^{-13}	2.90×10^{-13}
235	2.67×10^{-13}	2.66×10^{-13}
250	2.39×10^{-13}	2.38×10^{-13}
259	2.25×10^{-13}	2.23×10^{-13}
260	2.23×10^{-13}	2.21×10^{-13}
265	2.15×10^{-13}	2.14×10^{-13}
270	2.08×10^{-13}	2.07×10^{-13}
278	1.97×10^{-13}	1.97×10^{-13}
280	1.95×10^{-13}	1.94×10^{-13}
290	1.83×10^{-13}	1.82×10^{-13}
298	1.75×10^{-13}	1.74×10^{-13}
300	1.73×10^{-13}	1.72×10^{-13}
310	1.62×10^{-13}	1.61×10^{-13}
320	1.54×10^{-13}	1.53×10^{-13}
350	1.32×10^{-13}	1.30×10^{-13}
400	1.04×10^{-13}	1.03×10^{-13}

Table S8: The rate constant values for $\text{HOSO}^\bullet + \text{O}_2$ (${}^3\Sigma_g^-$) reaction through TS2 using TST/ZCT method. The values are given in $\text{cm}^3 \text{molecule}^{-1} \text{s}^{-1}$.

T(K)	k_{TST}	ZCT	k_{TST}/ZCT
213	4.10×10^{-32}	9.35×10^2	3.83×10^{-29}
216	7.29×10^{-32}	6.84×10^2	4.98×10^{-29}
219	1.28×10^{-31}	5.08×10^2	6.49×10^{-29}
224	3.14×10^{-31}	3.21×10^2	1.01×10^{-28}
235	2.00×10^{-30}	1.35×10^2	2.70×10^{-28}
250	1.92×10^{-29}	5.35×10^1	1.03×10^{-27}
259	6.61×10^{-29}	3.45×10^1	2.28×10^{-27}
260	7.55×10^{-29}	3.30×10^1	2.49×10^{-27}
265	1.44×10^{-28}	2.67×10^1	3.85×10^{-27}
270	2.68×10^{-28}	2.21×10^1	5.92×10^{-27}
278	6.94×10^{-28}	1.68×10^1	1.17×10^{-26}
280	8.73×10^{-28}	1.58×10^1	1.38×10^{-26}
290	2.62×10^{-27}	1.19×10^1	3.13×10^{-26}
298	6.00×10^{-27}	9.85×10^0	5.91×10^{-26}
300	7.34×10^{-27}	9.42×10^0	6.91×10^{-26}
310	1.92×10^{-26}	7.70×10^0	1.48×10^{-25}
320	4.76×10^{-26}	6.47×10^0	3.08×10^{-25}
350	5.33×10^{-25}	4.34×10^0	2.31×10^{-24}
400	1.37×10^{-23}	2.86×10^0	3.92×10^{-23}

Table S9: The relative energy and ZPE value of TS1 (in kcal mol^{-1}) with respect to RC at different level of theories. [a]; after including post-CCSD(T) corrections (table 1 in the manuscript), [b]; ZPE values obtained at MN15L/aug-cc-pV(T+d)Z level of theory.

Species	CCSD(T)/CBS	Post-CCSD(T) ^a	MRCI+Q/6-311G**	ZPE ^b
TS1	0.64	0.57	0.63	-1.91